



Version: 3.46

Search for leptonic jets and \cancel{E}_T in $p\bar{p}$ collisions at $\sqrt{s} = 1.96$ TeV

The DØ Collaboration
URL <http://www-d0.fnal.gov>
(Dated: June 28, 2010)

We present the first search for pair production of isolated jets of leptons in association with large missing transverse energy (\cancel{E}_T) at a hadron collider, using 5.8 fb^{-1} of D0 Run II data. No excess above multijet backgrounds is observed. Upper limits are set on the production cross section for supersymmetric (SUSY) chargino and neutralino pairs where the lightest SUSY particle decays into hidden sector particles giving jets of leptons and \cancel{E}_T , as a function of the dark photon mass.

Preliminary Results for BOOST 2010

I. INTRODUCTION

Hidden valley models [1] introduce a new, hidden sector, very weakly coupled to the standard model (SM) particles. Recently, these types of models with light particles in the hidden sector have been shown to give a cohesive interpretation [2, 3] of astrophysical [4–6] and direct dark matter search anomalies [7, 8]. High energy colliders may be able to produce these new particles [9–13]. Although details of the hidden sector can change the phenomenology significantly, several common features have emerged. The force carrier in the hidden sector, the dark photon (γ_D), must have a mass below ~ 2 GeV and generally decays into SM charged fermion (or pion) pairs. In many models the γ_D lifetime is small, and it does not travel an observable distance before decaying.

If R-parity conserving supersymmetry (SUSY) is realized, the lightest SUSY particle in the SM sector (SMLSP) can promptly decay into particles in the hidden sector. D0 has previously reported [14] on a search where this decay can give rise to either a photon or γ_D . However, the SMLSP could decay predominantly into the hidden sector, producing two or more dark particles in each event, see Figure 1. Pair produced hidden sector particles could also occur through rare decays of Z and Higgs boson(s) [13]. Single dark photons could also be directly produced, analogous to prompt SM photon production, in association with a QCD jet. However, this process is difficult to detect at a hadron collider, and analyses from higher luminosity, lower energy machines should be more sensitive [15, 16].

Since the hidden particles are light and highly boosted, decays into the hidden sector result in jets of tightly collimated particles from γ_D decays. If $m(\gamma_D) < 2 \cdot m(\pi^\pm)$, the jets consist exclusively of leptons. Even for larger γ_D masses the lepton content of the jets is high, so we refer to them as leptonic jets (l-jets). Every SUSY event in this scenario will have at least two l-jets and large \cancel{E}_T , from the LSP in the hidden sector (\tilde{X}). Radiation in the hidden sector [9] can dilute the l-jet signature; particles in the l-jets become softer, less tightly collimated, and less isolated.

In this Letter, we present the first search for events with two l-jets and large \cancel{E}_T at a hadron collider. Investigation of possible hidden sector signatures without significant \cancel{E}_T is left for future analyses. Data from Run II of the Fermilab Tevatron Collider recorded with the D0 detector [17] are used, corresponding to an integrated luminosity of about 5.8 fb^{-1} .

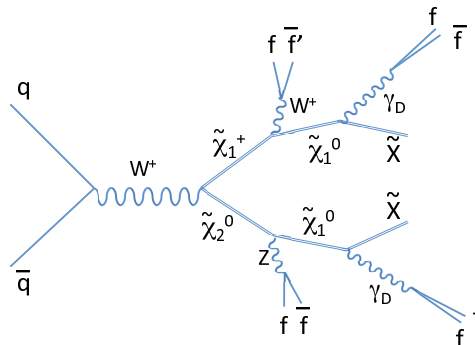


FIG. 1: A Feynman diagram of chargino + neutralino production, with decays into SMLSPs, which then decay into hidden sector SUSY particles (\tilde{X}) and dark photons (γ_D).

II. LEPTONIC JET SELECTION

Depending whether the γ_D of highest p_T decays to muons or electrons, the l-jet can appear as a “muon l-jet” or “electron l-jet” in the detector. To reconstruct muon l-jets, we start by demanding a muon track candidate with consistent hits in all three muon system layers matched to a central track with $p_T > 10$ GeV. Electron l-jets must have a track with $p_T > 10$ GeV spatially matched to an EM cluster within $\mathcal{R} = \sqrt{(\Delta\eta)^2 + (\Delta\phi)^2} < 0.2$ [18] with $E > 15$ GeV and not be already reconstructed as a muon l-jet. EM clusters are built using the simple cone algorithm of radius $\mathcal{R} = 0.4$, by requiring that the fraction of the energy deposited in the EM section of the calorimeter, EM_{frac} , is above 95% and the calorimeter isolation variable $\mathcal{I}_e = [E_{tot}(0.4) - E_{EM}(0.2)]/E_{EM}(0.2)$ is less than 0.2, where $E_{tot}(0.4)$ is the total energy in a cone of radius $\mathcal{R} = 0.4$, corrected for the underlying event contribution, and $E_{EM}(0.2)$ is the EM energy in a cone of radius $\mathcal{R} = 0.2$, which is taken to be the EM cluster energy. The seed track is required to have at least one hit in the silicon detector. The seed for any new l-jet must also be $\mathcal{R} > 0.8$ from the seed of any other previously found l-jet candidate in the same event. Next, a companion track of opposite charge from the seed track

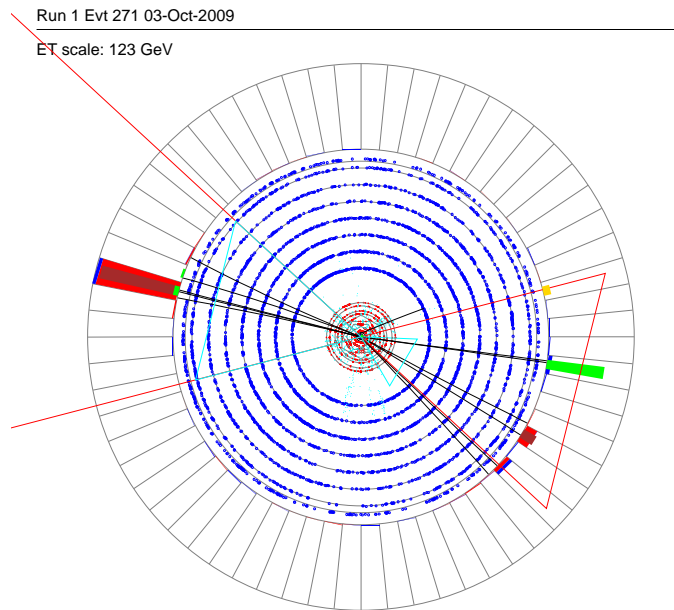


FIG. 2: A MC signal event, with a muon l-jet and an electron l-jet.

originating from a z position along the beamline within 1 cm from the seed track, and with $p_T > 4$ GeV is required within $\mathcal{R} < 0.2$ of the seed track. If more than one such track exists, the closest in \mathcal{R} is chosen.

We exploit the tight collimation of l-jets to distinguish them from the large (mostly heavy flavor) multijet background using track and calorimeter isolation. Track isolation is defined as the scalar sum of all track p_T in the area $0.2 < \mathcal{R} < 0.4$ from the seed track with $p_T > 0.5$ GeV and z within 1 cm from the seed track. Muon l-jet calorimeter isolation, \mathcal{I}_μ , follows [19], where the transverse energies of all calorimeter cells within $\mathcal{R} < 0.4$ are added, excluding cells within $\mathcal{R} < 0.1$ of either the seed muon or companion track. For electron l-jet isolation we employ the EM cluster isolation, \mathcal{I}_e .

Events are required to have at least two l-jet candidates of either the muon or electron type, and the three classes, $\mu\mu$, μe , and ee are analyzed separately. Each event (in data and MC) is allowed in just one class, with preference given to $\mu\mu$, then μe , then ee , since muon l-jets have less background. All recorded events are used, but most events selected have passed a single or di-lepton trigger [17]. Trigger efficiency is $>90\%$ for signal events passing the offline selections.

The main backgrounds are multijet events and, for electron l-jets, direct photon production with subsequent conversion to e^+e^- . Estimates of these backgrounds from simulations are highly unreliable, so they are determined from data. It is critical that the l-jet isolation requirements do not bias the kinematics of the background, such as the \cancel{E}_T or l-jet p_T 's, otherwise the background will be difficult to estimate. Isolation in the tracker for both muon and electron l-jets is required to be below 2 GeV, which does not significantly bias the background kinematics. We then tune l-jet calorimeter isolation requirements so they also do not bias the kinematics of the background. The isolation cuts are chosen as linear functions of l-jet p_T , such that the fraction of rejected background is large but minimally dependent on \cancel{E}_T . For EM objects we choose $\mathcal{I}_{EM} < 0.085 \cdot p_T - 0.53$, which rejects 90% of background. For muon l-jets we take the scalar sum of the muon and companion track p_T as the measure of the l-jet p_T , and the chosen cut is $\mathcal{I}_\mu < 0.066 \cdot p_T + 2.35$, which rejects 94% of the background. To verify that the rejections of these isolation cuts do not depend on the \cancel{E}_T , we compare the \cancel{E}_T distribution in the sample with just one isolated l-jet to the total (non-isolated) two l-jet sample. The two shapes are very close, which indicates that the kinematic bias is small. We can therefore use the shape of the \cancel{E}_T distribution in the non-isolated sample to predict the background shape in the sample with two isolated l-jets, which is still dominated by the same multijet processes.

Finally, we require $\cancel{E}_T > 30$ GeV, where \cancel{E}_T is calculated using the calorimeters only and not corrected for muons, since muon reconstruction is unreliable in l-jets due to the nearby tracks. We scale the \cancel{E}_T distribution in the non-isolated data sample so the total number of events with $\cancel{E}_T < 15$ GeV matches that in the isolated data sample, see Figure 3. If the track multiplicity in the l-jet is not large, the leading track and its companion track are likely to come from the decay of the same dark photon, so we also examine the invariant mass of the seed and companion track for events selected in the three high \cancel{E}_T analysis channels above (Figure 4).

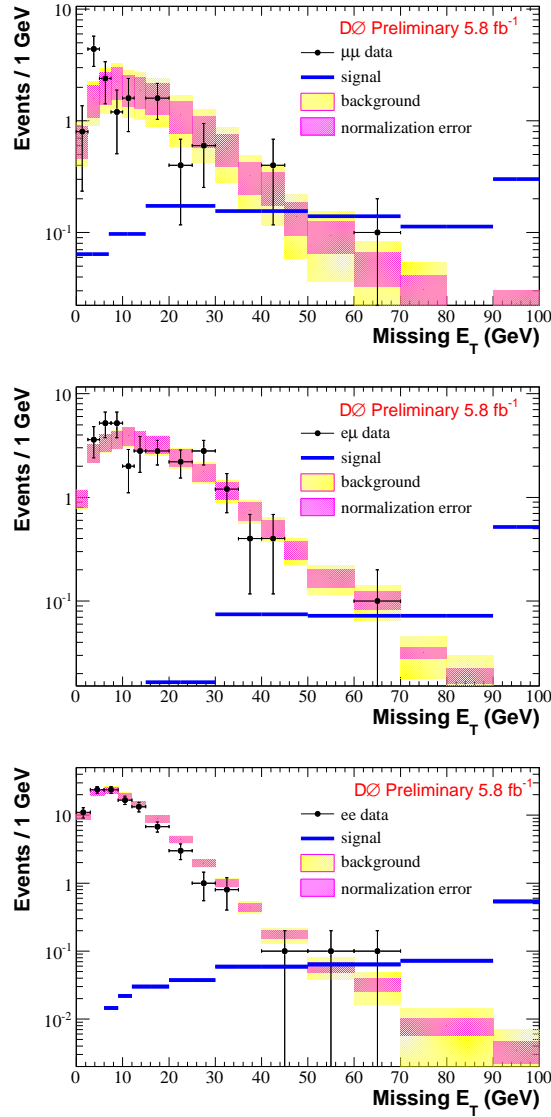


FIG. 3: The \cancel{E}_T distribution in events with two isolated muon l-jets (top), a muon and electron l-jet (middle), or two electron l-jets (bottom) is shown with black points. The shaded bands represents the expected backgrounds, with purple showing the correlated part of the systematic uncertainty from normalization and yellow the full uncertainty. The SPS8 signal MC distribution (see text) is scaled to have an integrated content of 10 events. The highest bin contains all events with $\cancel{E}_T > 100$ GeV as well.

III. SIMULATION

MadGraph [20] with Pythia [21] showering and hadronization was used to simulate signal events, which were processed with the full GEANT3-based [22] D0 detector simulation and event reconstruction. SUSY events with the SPS8 [23] parameters (a GMSB model) were generated as a benchmark. Production is dominated by lightest chargino pairs and lightest chargino in association with second neutralino, which cascade to the lightest neutralino (SMLSP), through decays involving either $W/Z/h$ bosons or sleptons. The cross section is ~ 20 fb, but the l-jet kinematics and thus detection efficiency would be very similar for other allowed points in SUSY parameter space with slightly lighter charginos and neutralinos, thus higher cross sections. The efficiency to reconstruct many tightly collimated tracks is hard to verify with real data. Therefore as a baseline model we consider the case where neutralinos decay only into a dark photon and a dark gaugino LSP (\tilde{X}) with mass of 1 GeV, which escapes as \cancel{E}_T . More complicated hidden sector scenarios are studied using MC simulation and discussed below.

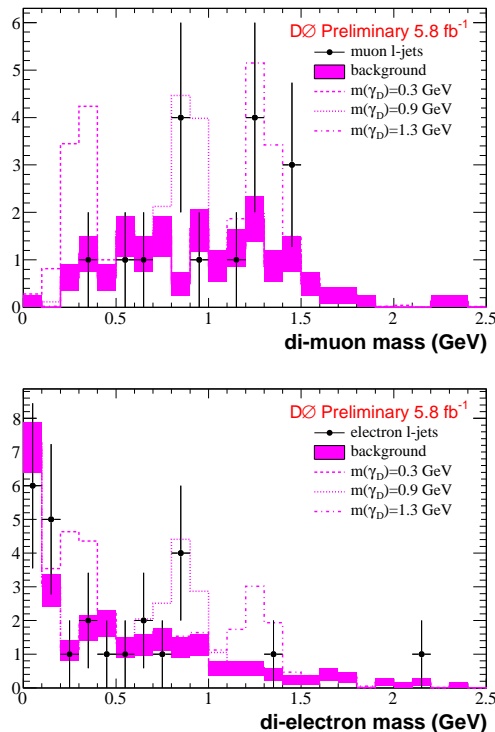


FIG. 4: Invariant mass of dark photon candidates with two isolated l-jets and $\cancel{E}_T > 30$ GeV, for muon (top) and electron (bottom) l-jets. Each candidate event contributes two entries, one for each l-jet. The purple band shows the mass distribution for events with $\cancel{E}_T < 20$ GeV, normalized to the number of entries with $\cancel{E}_T > 30$ GeV. The lines show the shape of MC signals, arbitrarily scaled to an integrated content of 8 events, for $m(\gamma_D) = 0.3, 0.9,$ and 1.3 GeV.

TABLE I: Events observed and expected from background for each channel, acceptance for the chosen SPS8 SUSY MC point, the reconstruction efficiency, and the total efficiency. The systematic uncertainty on the total efficiency is 20%.

Channel	Data	Background	SPS8 Acc.	Reco. eff.	Total eff.
ee	7	10.2 ± 1.7	0.45	0.20	8.9 %
$e\mu$	11	17.5 ± 4.2	0.53	0.15	7.8 %
$\mu\mu$	3	8.6 ± 4.5	0.50	0.12	5.8 %

IV. RESULTS

We split the detection efficiency into three parts (see Table I). First, the probability for an event to have at least two l-jets in a given combination (i.e. ee , $e\mu$, or $\mu\mu$), derived from the γ_D branching fractions [14]. Second, the acceptance for both l-jets to have the seed and companion tracks within $|\eta| < 1.1$ for electrons and 1.6 for muons and with $p_T > 10$ and 4 GeV, respectively, and true \cancel{E}_T , calculated as the vector sum of transverse momenta of all stable MC particles in the hidden sector, neutrinos, and muons, above 30 GeV. Third, the efficiency to reconstruct both l-jets in acceptance, pass isolation for both l-jets, and have reconstructed \cancel{E}_T in excess of 30 GeV. The acceptance and reconstruction efficiency did not vary significantly with $m(\gamma_D)$.

Since no excess of events is observed above expected backgrounds at large \cancel{E}_T , limits on l-jet production cross section are calculated, using a Bayesian approach with a flat prior for the signal cross section [24]. Limits are calculated separately for ee , $e\mu$, or $\mu\mu$ channels using the observed number of events, predicted background, and the detection efficiency and acceptance, see Figure 5. Systematic uncertainties are also included for the signal efficiency (20%), background normalization (20-50%), and luminosity (6.1%). The signal efficiency uncertainty is driven by our ability to verify the tracking efficiency for very nearby tracks in data. The background uncertainty is dominated by the remaining kinematic bias on \cancel{E}_T from the isolation cuts. Cross section limits are also calculated using the l-jet mass windows as shown in Table II. The backgrounds are normalized by scaling the events with $\cancel{E}_T < 20$ GeV to data,

TABLE II: Mass windows for the resonance search, with efficiencies for electron and muon l-jets to be within the windows, after all other selections. Also shown is the BR into electrons and muons for each dark photon mass.

$m(\gamma_D)$ (GeV)	BR(ee)($\mu\mu$)	M_{reco}^{low} - M_{reco}^{high} (GeV)	Eff. e	Eff. μ
0.15	1 0	0.0 - 0.3	0.81	-
0.3	0.53 0.47	0.1 - 0.4	0.82	0.88
0.5	0.4 0.4	0.3 - 0.6	0.81	0.89
0.7	0.15 0.15	0.4 - 0.8	0.85	0.89
0.9	0.27 0.27	0.6 - 1.1	0.82	0.91
1.3	0.31 0.31	0.9 - 1.4	0.72	0.79
1.7	0.22 0.22	1.0 - 1.8	0.73	0.76
2.0	0.24 0.24	1.3 - 2.2	0.73	0.83

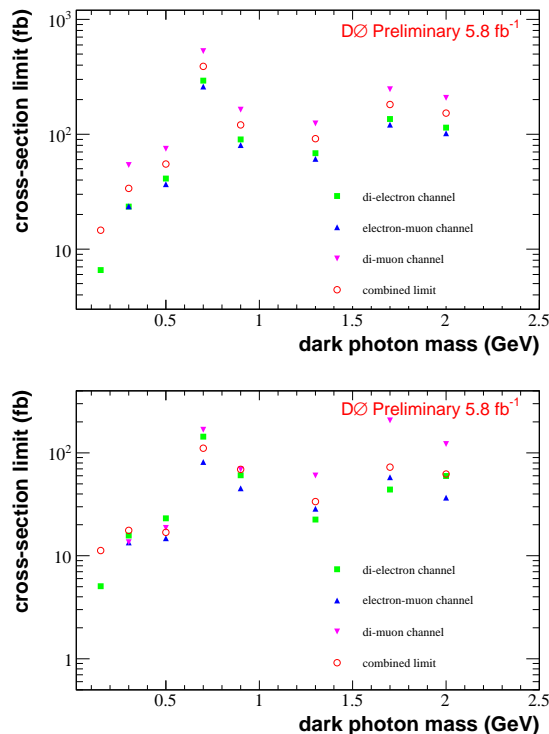


FIG. 5: Top: Cross section limits for individual channels (ee , $e\mu$, and $\mu\mu$) for acceptance of 1, and combined limits corrected for SPS8 acceptance from Table I. Bottom: Cross section limits from also using the measured invariant masses of the seed and companion tracks in both l-jets.

outside of the mass windows. The limit calculation method is not suitable in cases where the background is determined with an uncertainty of $\gtrsim 30\%$, so in these cases we conservatively take the expected background to be zero.

The dependence of the l-jet reconstruction and identification efficiency on several parameters of the hidden sector was studied using MC simulation, for muon and electron l-jet flavors. Additional MC samples were produced where the neutralino decays into a dark Higgs boson which then decays into two dark photons (see Figure 6b), leading to more, but softer, leptons in the l-jets. Efficiency in these samples was unaffected at small $m(\gamma_D)$, but up to 50% lower at large $m(\gamma_D)$, for both electron and muon l-jets (see Figure 7). The point $m(\gamma_D)=0.7$ also had 50% lower efficiency, due to the large pion branching fraction. MC was also produced with additional radiation in the hidden sector (see Figure 6a). Raising the dark coupling, α_D , from 0 to 0.3 reduced efficiency by up to 20%, independent of $m(\gamma_D)$. These efficiencies suffer high uncertainties since it is difficult to verify the detector simulation's accuracy for multi-track l-jets. However, it is encouraging that according to the MC simulation, the l-jet identification criteria maintain efficiency even for more complicated hidden sector behavior.

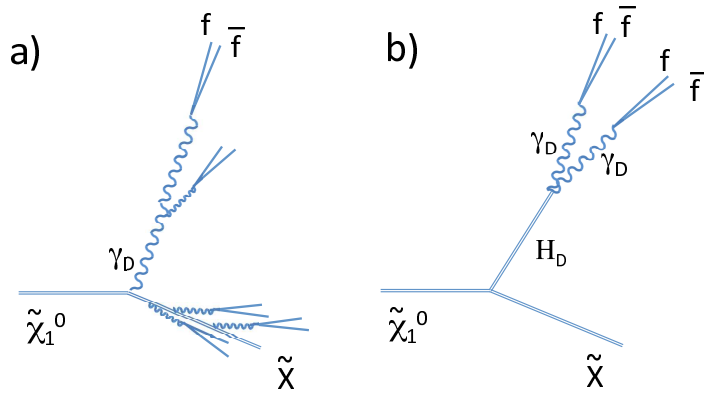


FIG. 6: **a)** Neutralino decay with extra radiation in the hidden sector around the \tilde{X} and dark photon. **b)** Neutralino decay into a dark Higgs boson, which then decays to dark photons, all of which forms a single l-jet.

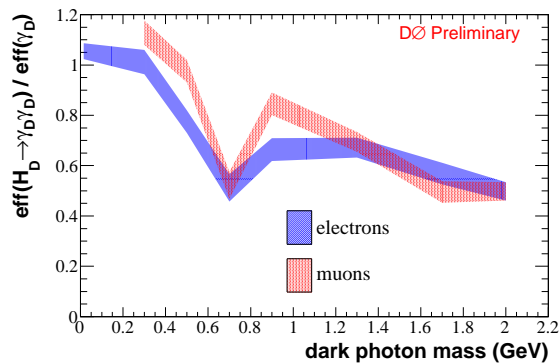


FIG. 7: Ratio of total efficiency for H_D l-jets to the standard γ_D l-jet total efficiency vs. $m(\gamma_D)$, for electron (blue band) and muon (red band) l-jets. Dark Higgs boson (H_D) decays produce l-jets with more particles and are wider.

V. SUMMARY

We performed a search for events with two tightly collimated jets of mainly leptons and large missing transverse energy using 5.8 fb^{-1} of data. The invariant mass of the l-jets, formed by the seed track and companion track, was also searched for a resonance. No evidence for these signals was observed, and upper limits were set on the production cross-section of SUSY events decaying to two l-jets with \cancel{E}_T , as a function of $m(\gamma_D)$.

We thank the staffs at Fermilab and collaborating institutions, and acknowledge support from the DOE and NSF (USA); CEA and CNRS/IN2P3 (France); FASI, Rosatom and RFBR (Russia); CNPq, FAPERJ, FAPESP and FUNDUNESP (Brazil); DAE and DST (India); Colciencias (Colombia); CONACyT (Mexico); KRF and KOSEF (Korea); CONICET and UBACyT (Argentina); FOM (The Netherlands); STFC and the Royal Society (United Kingdom); MSMT and GACR (Czech Republic); CRC Program and NSERC (Canada); BMBF and DFG (Germany); SFI (Ireland); The Swedish Research Council (Sweden); and CAS and CNSF (China). We also thank A. Falkowski, J. Ruderman, M. Strassler, S. Thomas, I. Yavin, and J. Wacker for many useful discussions and guidance.

-
- [1] T. Han, Z. Si, K. Zurek, and M. Strassler, JHEP **0807**, 008 (2008); M. Strassler and K. Zurek, Phys. Lett. B **651**, 374 (2007).
 - [2] D. P. Finkbeiner and N. Weiner, Phys. Rev. **D76** 083519 (2007).
 - [3] N. Arkani-Hamed, D. P. Finkbeiner, T. R. Slatyer, N. Weiner, Phys. Rev. **D79** 015014 (2009).
 - [4] A. A. Abdo *et al.*, Phys. Rev. Lett. **102**, 181101 (2009).

- [5] O. Adriani *et al.*, Nature **458**, 607 (2009).
- [6] J. Chang *et al.*, Nature **456**, 362 (2008).
- [7] R. Bernabì *et al.*, (DAMA/LIBRA Collaboration), Eur. Phys. J. C **56**, 333 (2008).
- [8] Z. Ahmed *et al.*, (CDMS II Collaboration), Science **327** (5973), 1619-1621 (2010).
- [9] M. Baumgart, C. Cheung, J. T. Ruderman, L.-T. Wang, I. Yavin, JHEP 0904:014, 2009.
- [10] D. S.M. Alves, S. R. Behbahani, P. Schuster, J. G. Wacker, arXiv:0903.3945v2 [hep-ph].
- [11] G. D. Kribs, T. S. Roy, J. Terning, K. M. Zurek, arXiv:0909.2034v1 [hep-ph].
- [12] A. Katz, Raman Sundrum, JHEP 0906:003, (2009).
- [13] A. Falkowski, J. T. Ruderman, T. Volansky, J. Zupan, arXiv:1002.2952 [hep-ph].
- [14] V. M. Abazov *et al.* (D0 Collaboration), Phys. Rev. Lett. **103**, 081802, (2009).
- [15] B. Aubert *et al.* (BaBar Collaboration), arXiv:0908.2821v1. B. Aubert *et al.* (BaBar Collaboration), Phys. Rev. Lett. **103**, 081803 (2009).
- [16] J. D. Bjorken, R. Essig, P. Schuster, N. Toro, Phys. Rev. **D80** 075018 (2009).
- [17] V. Abazov *et al.* (D0 Collaboration), Nucl. Instrum. Methods Phys. Res. A **565**, 463 (2006).
- [18] The D0 detector utilizes a right-handed coordinate system with the z -axis pointing in the direction of the proton beam and the y -axis pointing upwards. The azimuthal angle ϕ is defined in the xy plane measured from the x -axis. The pseudorapidity is defined as $\eta = -\ln[\tan(\theta/2)]$, where $\theta = \arctan(\sqrt{x^2 + y^2}/z)$.
- [19] V. M. Abazov *et al.* [D0 Collaboration], Phys. Rev. Lett. **103**, 061801 (2009) [arXiv:0905.3381 [hep-ex]].
- [20] J. Alwall *et al.*, JHEP **0709**, 028 (2007) [arXiv:0706.2334 [hep-ph]].
- [21] T. Sjöstrand *et al.*, Comput. Phys. Commun. **135**, 238 (2001).
- [22] R. Brun and F. Carminati, CERN Program Library Long Writeup W5013, 1993 (unpublished).
- [23] The neutralino mass for this SUSY point is ~ 140 GeV and the second neutralino / chargino masses are both ~ 265 GeV. S.P. Martin, S. Moretti, J.M. Qian, and G.W. Wilson, "Direct Investigation of Supersymmetry: Subgroup summary report," in *Proceedings of the APS/DPF/DPB Summer Study on the Future of Particle Physics (Snowmass 2001)*, edited by N. Graf, eConf **C010630**, p. 346 (2001); B.C. Allanach *et al.*, Eur. Phys. J. C **25**, 113 (2002).
- [24] I. Bertram *et al.* FERMILAB-TM-2104.

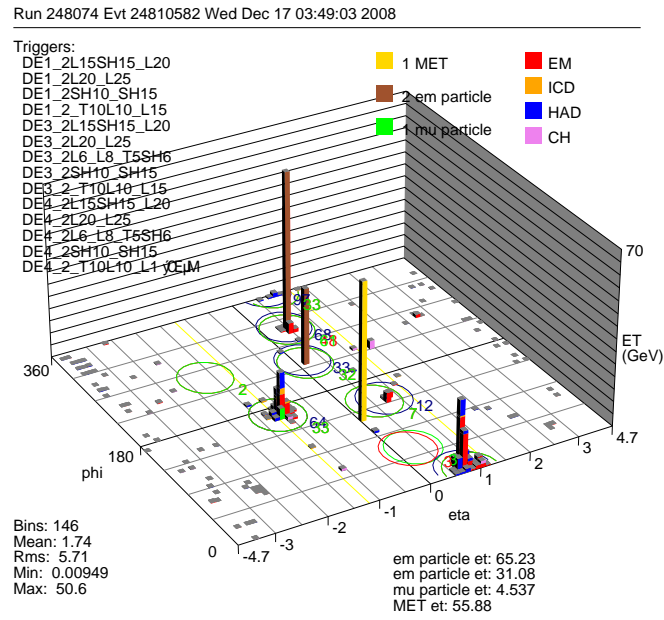


FIG. 8: Lego view of a two electron l-jet candidate event in data with large \cancel{E}_T .

Run 248074 Evt 24810582 Wed Dec 17 03:49:03 2008

ET scale: 52 GeV

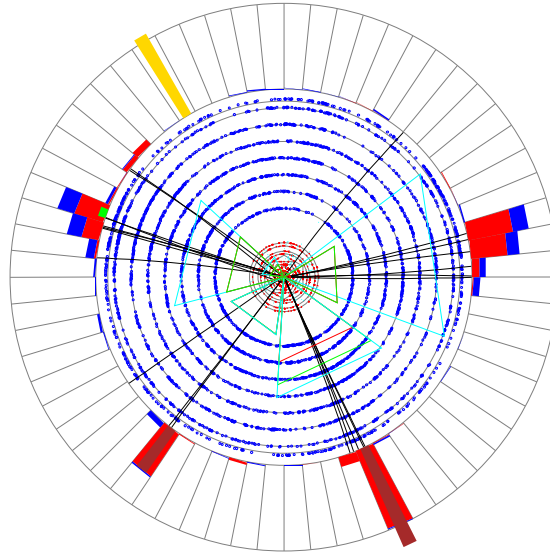


FIG. 9: XY view of a two electron l-jet candidate event in data with large \cancel{E}_T .

VI. APPENDIX A

Figures 8-10 show a candidate event in data with two isolated electron l-jets and large \cancel{E}_T .

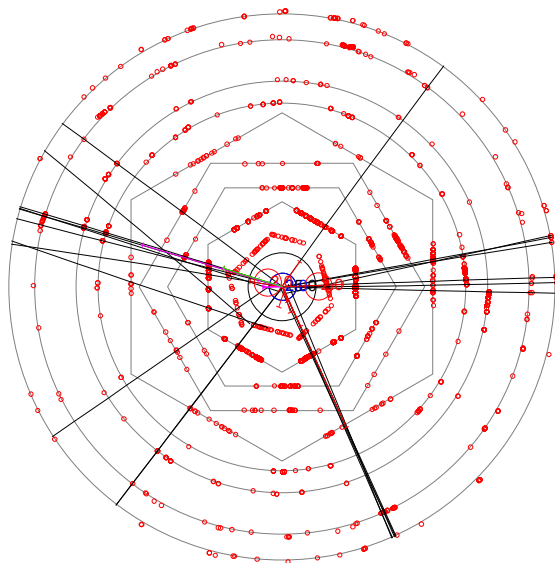


FIG. 10: Zoom XY view of a two electron l-jet candidate event in data with large \cancel{E}_T .